Chaotic Modeling and Simulation (CMSIM) 2: 223–234, 2017

Synchronization of Small-World Networks with Multi-Scroll Chaotic Oscillators

A.G. Soriano-Sánchez[1], C. Posadas-Castillo[1], M.A. Platas-Garza[1], C. Cruz-Hernández[2], and A.E. Loya-Cabrera[1]

[1] Universidad Autónoma de Nuevo León – Facultad de Ingeniería Mecánica y Eléctrica, N.L, México
(E-mail: allansori@gmail.com, cornelio.posadascs@uanl.edu.mx, miguel.platasg@uanl.mx, aloya67@gmail.com)

[2] Electronics and Telecommunications Department (CICESE)
Carretera Ensenada – Tijuana No.3918, Zona Playitas, C.P. 22860 Ensenada, B.C., México
(E-mail: ccruz@cicese.mx)

Abstract. In this paper, authors study the synchronization of a small-world network. We consider chaotic generators of multi-scroll attractor to compose the complex network. By applying Newman-Watts algorithm, we introduce long-range connections in an arrangement of N-coupled chaotic oscillators, attempting to improve communication between the oscillators. Authors will show that the small-world property allows us to synchronize a complex network by using a small coupling strength. Chaotic synchronization is achieved by using the complex systems theory. Numerical simulations are provided to show the effectiveness of the method.

Keywords: Chaos synchronization, small-world networks, multi-scroll chaotic attractors.

1 Introduction

The decade of the 1960's witnessed two of the most important findings on nonlinear and complex systems: we can firstly mention the emergence of chaotic behavior, being Edward N. Lorenz who presented the first evidence of chaos. Helped by the emerging computers, that made possible to visualize the behavior of some systems from the solution of their differential equations, Lorenz published his historical article on deterministic nonperiodic flow [1]. By using numerical methods, the trajectories of some equations, which described the forced dissipative hydrodynamic flow, were obtained to be identified in phase space. This resulted in the generation of a significant amount of knowledge, which led to a deep study of the field and the emergence of numerous systems exhibiting this phenomenon, from which can be highlighted conventional chaotic oscillators like Chua, Lorenz and Rössler [1–4], multi-scroll chaotic oscillators [5–8], fractional-order chaotic oscillators [9–11], for instance.

Received: 17 April 2016 / Accepted: 14 December 2016

ISSN 2241-0503

Thirty years later, chaos was again the center of attention after L.M. Pecora and T.L. Carroll synchronized, for the first time, two identical chaotic oscillators with different initial conditions [12]. In the years following this achievement, the basic concepts and applications of chaos synchronization were established. The most remarkable works on this field are the following:

C.W. Wu and L.O. Chua defined the concepts of asymptotic and partial synchronization in 1994, establishing the relation between asymptotic synchronization and asymptotic stability [13]. J.F. Heagy et al. investigated the role of unstable periodic orbits in synchronous chaotic behavior in 1995 [14], proving how desynchronized bursting behavior is initiated, and suggesting taking this phenomenon into account to yield high quality chaotic synchronization.

In 1996, N.F. Rulkov discussed the cooperative behavior related to the regimes of synchronized chaos and outlined some examples that illustrate different types of identical chaotic oscillations [15]. L.M. Pecora et al. reviewed the basics of chaotic synchronization and examined coupling configurations as well as secure communication schemes one year later [16]. A unified approach for the analysis and comparison of conventional and chaotic communications systems was provided by G. Kulumbán et al., who clarified the role of synchronization for chaotic communications and described chaotic synchronization schemes [17].

The second remarkable event of the 1960's, was the definition of the concept of *six degrees of separation*, derived from an experiment performed by Stanley Milgram [18,20]. According to [19,20], Milgram's experiment consisted of randomly distributed letters to people in Nebraska to be sent to Boston by people who might know the consignee. Milgram found that it had only taken an average of six steps for a letter to get from Nebraska to Boston. He concluded that six was the average number of acquaintances separating people in the entire world. This famous concept later evolved into the small-world property.

The small-world networks became popular after D.J. Watts and S.H. Strogatz published the algorithm to introduce the small-world property into a regular network. They showed the resulting network fulfilled high clustering coefficient and short average path length [19].

In this paper, we combine the complexity generated by nonlinear systems, which generate multi-scroll chaotic attractors for our case, and the properties of complex systems, whose topology is of great interest, which has been proved to have influence in two major results: firstly, the discovery that the behavior of biological and non-biological systems can be modeled by the dynamics of complex networks [21–27]. Secondly, the influence or effect of topology on the realization of system processes [28–30].

This work addresses the chaotic synchronization of a complex network that displays the small-world property, which will be introduced by using the Newman-Watts algorithm. Every element of the network will be a nonlinear dynamical system, which has the ability to generate multi-scroll chaotic attractors. Authors will show it is possible to carry the complex network to behave in a synchronous way by applying a control law only in one state and by using a relative small coupling strength.

The remainder of the paper is organized as follows: a brief review on complex dynamical networks and their synchronization is given in Sect. 2. Section 3 provides the explanation of the Newman-Watts small-world algorithm and the description of its basic characteristics. Section 4 provides the model description of the multi-scroll chaotic oscillator, which will be used to compose the complex network, and its corresponding chaotic attractor. Numerical simulations of an example of chaotic synchronization of a small-world network are provided in Sect. 5. The computation of the coupling strength is also provided here. Some conclusions are given in Sect. 6.

2 Complex Networks

In the present Sect. we will address the topic of complex networks and their synchronization. We will provide the definition of a complex network and the coupling matrix technique, which is used to achieve synchronization.

Among the possible definitions of a complex network, we will use the one suggested by Wang [31].

Definition 1. A complex network is defined as an interconnected set of oscillators (two or more), where each oscillator is a fundamental unit, with its dynamic depending of the nature of the network.

Each oscillator is defined as follows

$$\dot{\mathbf{x}}_i = f(\mathbf{x}_i) + \mathbf{u}_i \ , \qquad \mathbf{x}_i(0), \qquad i = 1,\ 2, \ldots,\ N, \tag{1}$$

where N is the network's size, $\mathbf{x}_i = [x_{i1},\ x_{i2},\ \ldots,\ x_{in}] \in \mathrm{I\!R}^{\mathrm{n}}$ represents the state variables of the oscillator i. $\mathbf{x}_i(0) \in \mathrm{I\!R}^{\mathrm{n}}$ are the initial conditions for oscillator i. $\mathbf{u}_i \in \mathrm{I\!R}^{\mathrm{n}}$ establishes the synchronization between two or more oscillators and it is defined as follows [32]

$$\mathbf{u}_i = c \sum_{j=1}^{N} a_{ij} \varGamma \mathbf{x}_j, \qquad i = 1,\ 2, \ldots,\ N. \tag{2}$$

The constant $c > 0$ represents the coupling strength. $\varGamma \in \mathrm{I\!R}^{\mathrm{n \times n}}$ is a constant matrix to determine the coupled state variable of each oscillator. Assume that $\varGamma = \mathrm{diag}(r_1,\ r_2, \ldots,\ r_n)$ is a diagonal matrix. If two oscillators are linked through their k-th state variables, then, the diagonal element $r_k = 1$ for a particular k and $r_j = 0$ for $j \neq k$.

Synchronization is achieve through (2), where a_{ij} are the elements of $A \in \mathrm{I\!R}^{\mathrm{N \times N}}$ which is the coupling matrix. The matrix A shows the connections between oscillators; if the oscillator i-th is connected to the oscillator j-th, then $a_{ij} = 1$, otherwise $a_{ij} = 0$ for $i \neq j$. The diagonal elements of A matrix are defined as

$$a_{ii} = - \sum_{j=1, j \neq i}^{N} a_{ij} = - \sum_{j=1, j \neq i}^{N} a_{ji}, \qquad i = 1, 2, ..., N. \tag{3}$$

The dynamical complex network (1)–(2) is said to achieve synchronization if

$$\mathbf{x}_1(t) = \mathbf{x}_2(t) = \ldots = \mathbf{x}_\mathrm{N}(t) \quad \text{as} \quad t \to \infty. \tag{4}$$

In this work we will synchronize N-coupled multi-scroll chaotic oscillators arranged in small-world topology.

3 Small–World Networks

The small-world property consists in the existence of long-range links connecting pairs of nodes distant from each other. The concept of the six degrees of separation is implied due to it is needed a small number of steps (acquaintances) to reach any node in this type of networks.

The complex network features that will be affected by the small-world property are: on one hand *the clustering coefficient* C, which is defined as the average fraction of pairs of neighbors of an oscillator that are also neighbors of each other, the clustering coefficient c_i of the oscillator i is defined as the ratio between the actual number E_i of edges that exist between k_i oscillators and the total number $k_i(k_i-1)/2$ [31,33], so $c_i = 2E_i/k_i(k_i-1)$. The clustering coefficient C of the whole network is the averaged of c_i over all i

$$C = \frac{1}{N}\sum_{i=1}^{N}\frac{2E_i}{k_i(k_i-1)}. \tag{5}$$

On the other hand *the average shortest path length* L, which is defined as the shortest distance between two oscillators averaged over all pairs of oscillators [31,33]

$$L = \frac{1}{N(N-1)}\sum_{i\neq j} d_{ij}, \qquad 1 \le i, j \le N, \tag{6}$$

where d_{ij} is the distance between node i and node j. Due to the existence of long-range links, the small-world network has high clustering coefficient $C(N,p)$ and short average path length $L(N,p)$.

In the following, the Newman-Watts algorithm, which is used to introduce the small-world property into a regular network, will be described.

3.1 Newman-Watts Small-World Algorithm

In 1998 D.J. Watts and S.H. Strogatz proposed the first algorithm to introduce the small-world property into a regular network. One year later M.E.J. Newman and D.J. Watts proposed a revised version of the original small-world algorithm [34,35]. The Newman-Watts procedure starts from the nearest neighbor topology, which is a ring lattice with periodic boundary conditions [35], but unlike the previous case, this algorithm introduces the small-world property by adding links to pairs of nodes, in this case chaotic oscillators, randomly chosen. Restrictions are:

1. The size of the networks remains unchanged.

2. No oscillator is allowed to have multiple links with other oscillator.
3. No oscillator is allowed to have links with itself.
4. It is strongly recommended to hold the relation $N \gg k$,

where N is the size of the network, k is the periodic boundary condition, i.e., the oscillator i is connected with its $i \pm 1, i \pm 2, \ldots, i \pm k$ neighboring oscillators; p is the probability to add a link. To determine the amount of links to be added we consider the following: the oscillator i is already connected with its $2k$ neighboring oscillators. The third restriction does not allow the oscillator i to have links with itself, thus, it can connect $N-(2k+1)$ oscillators more; therefore, for the whole network we have $N(N-(2k+1))$ links. However, since the considered network is undirected and the second restriction does not allow multiple links between pairs of oscillators, the connection from oscillator i to oscillator j is the same as the connection from oscillator j to oscillator i; therefore we have $N(N-(2k+1))/2$ possible links. As the Newman-Watts algorithm is applied, $N(N-(2k+1))p/2$ links are introduced.

Figure 1 shows the evolution of the Newman-Watts small-world algorithm. We conclude the following: when $p = 0$ the topology remains unchanged and the network is considered regular. As the probability increases $0 < p < 1$ one obtains a small-world network by adding links to randomly pairs of oscillators. At the point where $p = 1$ all the possible links have been added and the network has become globally coupled.

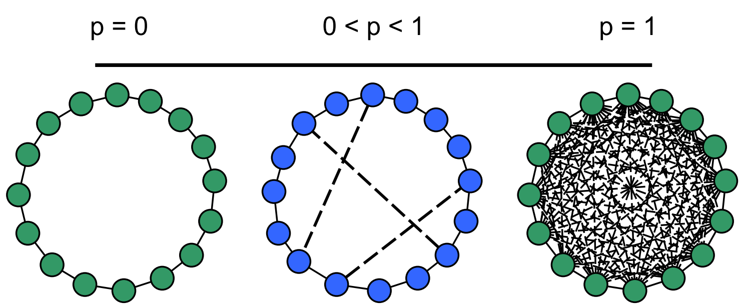

Fig. 1. Evolution of the Newman-Watts small-world algorithm. For $p = 0$ and $p = 1$ we obtain regular topologies; when $0 < p < 1$ one obtains small-world topology. The *solid* lines are the original links. The *dashed* lines are the links randomly added as p increases

Figure 2 depicts the evolution of the clustering coefficient C and the average shortest path length L, as the Newman-Watts small-world algorithm is applied in a network with $N = 200$ and $k = 20$. We want the reader to notice two things: on one hand, how the average shortest path length decreases significantly for a small change in the probability, reaching its lowest value for $p \approx 0$. On the other hand, the fact that the clustering coefficient, whose highest value for a network is $C = 1$, increases significantly for $p \approx 1$.

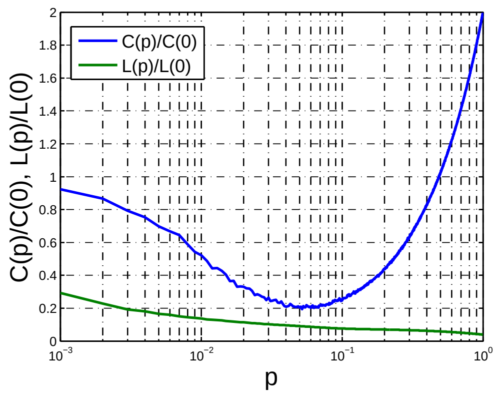

Fig. 2. Evolution of the clustering coefficient C and the average shortest path length L of a network with $N = 200$ and $k = 2$

In the following, we will present the model that describes the multi-scroll chaotic oscillator, which will be used to compose the small-world network to be synchronized.

4 Multi-Scroll Chaotic Oscillator Genesio-Tesi 3D

In this Sect., authors provide the mathematical model of the multi-scroll attractor generator, which is a generalization of the original Genesio-Tesi chaotic oscillator, that generates different amount of scrolls along any of its state variables. For simplicity, we will call it Genesio-Tesio 3D, which is described as follows [36]:

$$\begin{cases} \dot{x} = y - f_1(y), & f_1(y) = \sum_{i=1}^{M_y} g_{\frac{(-2i+1)}{2}}(y) + \sum_{i=1}^{N_y} g_{\frac{(2i-1)}{2}}(y), \\ \dot{y} = z - f_1(z), & f_1(z) = \sum_{i=1}^{M_z} g_{\frac{(-2i+1)}{2}}(z) + \sum_{i=1}^{N_z} g_{\frac{(2i-1)}{2}}(z), \\ \dot{z} = -ax - ay - az + af_3(x), & f_3(x) = \sum_{l=1}^{m-1} \gamma g_{n_l}(x), \end{cases} \tag{7}$$

where $n_l = \rho + 0.5 + (l-1)(\rho + \varsigma + 1)$, $\gamma = \rho + \varsigma + 1$, $\rho = |\min_{i,j}\{u_i^{eq,y} + u_j^{eq,z}\}|$, $\varsigma = |\max_{i,j}\{u_i^{eq,y} + u_j^{eq,z}\}|$ and

$$g_\theta(\bullet) = \begin{cases} 1, & \bullet \geq \theta, \theta > 0, \\ 0, & \bullet < \theta, \theta > 0, \\ 0, & \bullet \geq \theta, \theta < 0, \\ -1, & \bullet < \theta, \theta < 0. \end{cases} \tag{8}$$

Here, x, y, $z \in \mathbb{R}$; $a = 0.8$ makes (7) to exhibit chaotic behavior. $u^{eq,y} = -M_y, \ldots, -1, 0, 1, \ldots, N_y$ and $u^{eq,z} = -M_z, \ldots, -1, 0, 1, \ldots, N_z$, are the vectors for the y and z variables related to the equilibrium points and (8) is the core function [36]. In Fig. 3**a** it is shown an example of the time evolution of the $y(t)$ state variable. Figure 3**b** depicts a modality of Genesio-Tesi 3D chaotic attractor with $4 \times 2 \times 2$ scrolls.

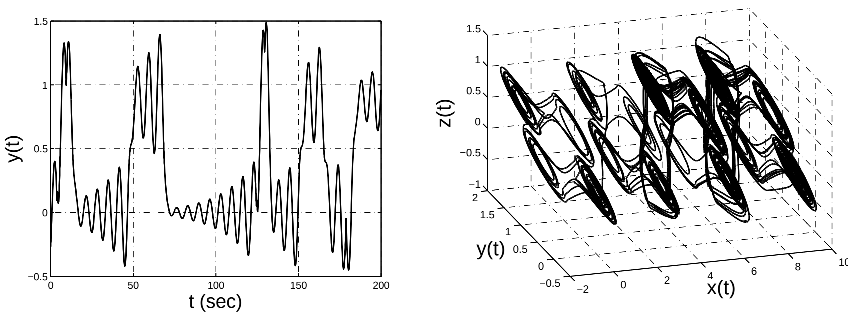

(a) (b)

Fig. 3. (**a**) Time evolution of $y(t)$ state variable obtained with (7). (**b**) View $x-y-z$ of a $4 \times 2 \times 2$ multi-scroll chaotic attractor obtained with $[x(0),\ y(0),\ z(0)] = [-0.3,\ 0.5,\ -0.1]$, $M_y = 0$, $N_y = 1$, $M_z = 0$, $N_z = 1$ and $m = 4$ for $u^{eq,y} = [0\ 1]$ and $u^{eq,z} = [0\ 1]$

5 Synchronization results

In the following, complex networks of identical multi-scroll chaotic oscillators Genesio-Tesi 3D will be synchronized.

Considering a synchronization scheme of $N = 300$ chaotic oscillators, with periodic boundary condition $k = 10$, we obtain the coupling matrix of the nearest neighbor topology. Then, we apply the Newman-Watts algorithm to introduce the long-range connections to generate a small-world network, whose elements will be the multi-scroll chaotic generator Genesio-Tesi 3D. According to (1), the small-world network is described as follows

$$\begin{cases} \dot{x}_i = y_i - f_1(y_i) + c\sum_{j=1}^{N} a_{ij}x_i, \\ \dot{y}_i = z_i - f_1(z_i), & \text{for} \quad i = 1, \dots,\ N, \\ \dot{z}_i = -ax_i - ay_i - az_i + af_3(x_i), \end{cases} \tag{9}$$

where

$$f_1(y_i) = \sum_{n=1}^{M_y} g_{\frac{(-2n+1)}{2}}(y_i) + \sum_{n=1}^{N_y} g_{\frac{(2n-1)}{2}}(y_i), \tag{10}$$

$$f_1(z_i) = \sum_{n=1}^{M_z} g_{\frac{(-2n+1)}{2}}(z_i) + \sum_{n=1}^{N_z} g_{\frac{(2n-1)}{2}}(z_i), \tag{11}$$

$$f_3(x_i) = \sum_{l=1}^{m-1} \gamma g_{n_l}(x_i), \quad (12)$$

using the core function (8) for each nonlinearity $f_1(\bullet)$ and n_l, γ, ρ, ς as previously described.

As we can remember from Sect. 2, the control law, given by (2), depends on Γ matrix, set as $\Gamma = \mathrm{diag}(1,\ 0,\ 0)$, that means we couple through the first state; the coupling matrix elements a_{ij} and the coupling strength c. The latter will be obtained by using a methodology, originally designed for other types of networks [23], to investigate its effectiveness in achieving synchronization on small-world networks.

Consider the small-world network described by (9). The synchronization error between any pair of chaotic oscillators will be defined as $e_1 = x_1 - x_2$, $e_2 = y_1 - y_2$ and $e_3 = z_1 - z_2$, that yields the following synchronization error system

$$\begin{cases} \dot{e}_1 = -2ce_1 + e_2 - [f_1(y_1) - f_1(y_2)], \\ \dot{e}_2 = e_3 - [f_1(z_1) - f_1(z_2)], \\ \dot{e}_3 = -ae_1 - ae_2 - ae_3 + a[f_3(x_1) - f_3(x_2)]. \end{cases} \quad (13)$$

As can be deduced, when (13) reaches equilibrium, the variables involved reach synchronization, this means:

$$\lim_{t\to\infty} \left\| [x_1\ y_1\ z_1]^T - [x_2\ y_2\ z_2]^T \right\| = 0. \quad (14)$$

By setting $\dot{e}_1 = \dot{e}_2 = \dot{e}_3 = 0$, one obtains the equilibrium point, whose stability is analyzed by using the following Lyapunov candidate function

$$V(e) = \frac{1}{2}(be_1^2 + 2e_1e_3 + be_2^2 + 2e_2e_3 + be_3^2), \qquad V(e) > 0 \text{ for } b > \sqrt{2}. \quad (15)$$

The matricial form of $\dot{V}(e) = \mathbf{e}^T Q \mathbf{e}$ evaluated along the trajectories of the synchronization error system (13), allows to show $\dot{V}(e)$ negative definiteness by showing Q positive definiteness. Therefore, if

$$Q = \begin{bmatrix} (2bc + a) & -\frac{1}{2}(b - 2a) & q_1 \\ -\frac{1}{2}(b - 2a) & a & q_2 \\ q_1 & q_2 & (ba - 1) \end{bmatrix}, \quad (16)$$

where

$$\begin{aligned} q_1 &= \tfrac{1}{2}(a + ba + 2c), \\ q_2 &= -\tfrac{1}{2}(1 + b - a - ba), \end{aligned} \quad (17)$$

we determine that 1st and 2nd principal minors of matrix Q, i.e., $(2bc + a) > 0$ and $a(2bc+a) - \frac{1}{4}(b-2a)^2 > 0$ for $c > 0$ so that, positive definiteness of matrix Q depends on its 3rd principal minor given by

$$\begin{aligned} |M_3| = &- \left(\tfrac{4}{5}\right) c^2 - \left(\tfrac{1}{50}b^3 - \tfrac{67}{50}b^2 + \tfrac{58}{25}b + \tfrac{4}{5}\right) c \\ &- \left(\tfrac{4}{25}b^3 - \tfrac{77}{100}b^2 + \tfrac{29}{25}b + \tfrac{1}{5}\right), \end{aligned} \quad (18)$$

for $a = 0.8$. Figure 4 shows the range of the coupling strength c as function of the parameter of the Lyapunov candidate function b to assure the positiveness

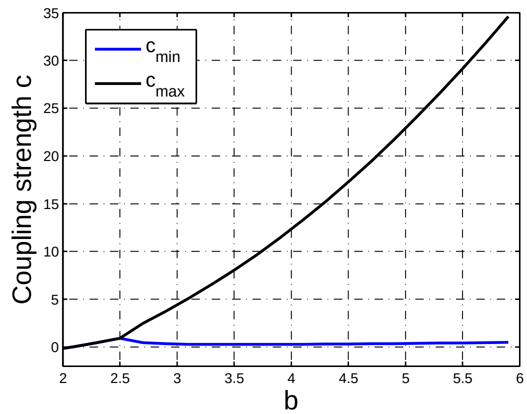

Fig. 4. Lower and upper boundary of the coupling strength c as function of the parameter b obtained from (18)

of M_3. By choosing the coupling strength within the range given, the stability of the synchronization error system (13) is guaranteed, thus, variables involved will synchronize. For further details on this procedure please refer to [23].

In the following, we will present the synchronization results of the small-world network (9), by applying the computed coupling strength, given in Fig. 4, to show it is big enough to take the network to behave in a synchronous way, but small enough to produce a less invasive control law. We assigned arbitrary initial conditions within the range $[-15,\ 15]$, and set the parameter $b = 5$ and the corresponding coupling strength at $c = 1$ with a probability $p = 0.3$ to produce the following synchronization results: Figure 5**a** shows the time evolution of $z(t)$ state variable of some chaotic oscillators randomly chosen. The time evolution of $e_2(t)$, which denotes the synchronization error between $y(t)$ states variables, is shown in Fig. 5**b** to confirm synchronization in the second state variable.

The phase portraits between $x(t)$ variables of some arbitrary chosen oscillators are shown in Fig. 6. The multi-scroll chaotic attractor of the final dynamic is embedded in Fig. 6 as well.

6 Conclusion

In this work the synchronization of complex networks with small-world topology, composed of multi-scroll chaotic oscillators was performed. Synchronization was accomplished by using the coupling matrix technique and by applying the control law only in one state. We highlight the fact that we computed the coupling strength by using a procedure originally designed for other types of networks, even though, we have shown it is possible to achieve synchronization in small-world networks by using it. It is worth mentioning that the analysis provides only sufficient stability conditions since it is based on the Lyapunov

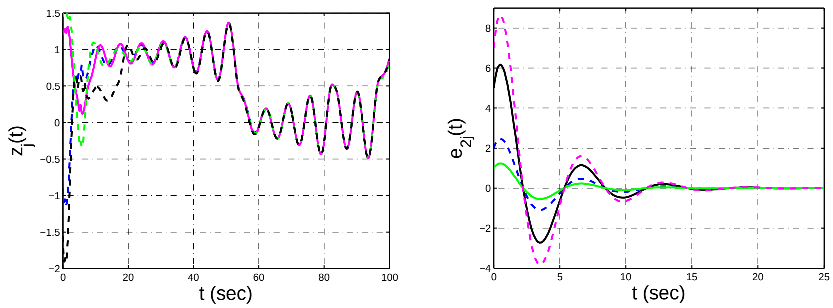

(a) (b)

Fig. 5. (**a**) Time evolution of state variables $z_j(t)$ for $j = 26,\ 53,\ 249,\ 130$, where synchronization can be observed. (**b**) Time evolution of $e_{2j}(t)$, which is the second state variable of the synchronization error system, where $j = 1,\ 2,\ 3,\ 4$ stands the following combinations $y_5(t) - y_{28}(t)$, $y_{10}(t) - y_{83}(t)$, $y_{32}(t) - y_{70}(t)$ and $y_4(t) - y_{96}(t)$

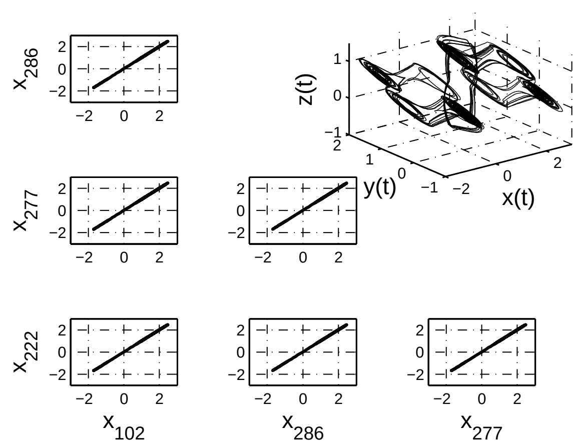

Fig. 6. Phase portraits between $x_i(t)$ vs $x_j(t)$ state variables of some arbitrary chosen chaotic oscillators, where $i = 102,\ 286,\ 277$ and $j = 286,\ 277,\ 222$. We confirm synchronization in $x(t)$ with a 45° line

method. Therefore, the range of the coupling strength c is not unique and other values that may lead the network to synchrony are not excluded.

7 Acknowledgement

This work was supported by CONACYT México under Research Grant No. 166654, PAICYT under Research Grant IT956-11 and Facultad de Ingeniería Mecánica y Eléctrica (FIME-UANL).

References

1. E. N. Lorenz. Deterministic Nonperiodic Flow. *Journal of the atmospheric sciences*, 20, 130–141, 1963.
2. L. O. Chua, M. Komuro and T. Matsumoto. The Double Scroll Family. *IEEE Transactions on Circuits and Systems*, 11, 1072–1118, 1986.
3. T. Matsumoto. A Chaotic Attractor from Chua's Circui. *IEEE Transactions on Circuits and Systems*, 31, 12, 1055–1058, 1984.
4. O. E. Rössler. An equation for continuous chaos. *Physics Letters A*, 57, 5, 397–398, 1976.
5. M. E. Yalçin. Multi–scroll and hypercube attractors from a general jerk circuit using Josephson junctions. *Chaos, Solitons & Fractals*, 34, 1659–1666, 2007.
6. J. Lu, S. Yu, H. Leung and G. Chen. Experimental Verification of Multidirectional Multiscroll Chaotic Attractors. *IEEE Transactions on Circuits and Systems I: Regular Papers*, 53, 1, 149–165, 2006.
7. J. Lu and G. Chen. Generating Multiscroll Chaotic Attractors: Theories, Methods and Applications. *International Journal of Bifurcation and Chaos*, 16, 4, 775–858, 2006.
8. E. Tlelo–Cuautle, J. J. Rangel–Magdaleno, A. D. Pano–Azucena, P. J. Obeso–Rodelo and J. C. Nunez-Perez. FPGA realization of multi–scroll chaotic oscillators. *Communications in Nonlinear Science and Numerical Simulation*, 27, 1, 66–80, 2015.
9. I. Petráš. A note on the fractional–order Chua's system. *Chaos, Solitons & Fractals*, 38, 1, 140–147, 2008.
10. X. Huang, Z. Zhao, Z. Wang and Y. Li. Chaos and hyperchaos in fractional–order cellular neural networks. *Neurocomputing*, 94, 13–21, 2012.
11. M. S. Tavazoei and M. Haeri. Chaotic attractors in incommensurate fractional order systems. *Physica D: Nonlinear Phenomena*, 237, 20, 2628–2637, 2008.
12. L. M. Pecora and T. L. Carroll. Synchronization in chaotic systems. *Physical review letters*, 64, 8, 821–824, 1990.
13. C. W. Wu and L. O. Chua. A unified framework for synchronization and control of dynamical systems. *International Journal of Bifurcation and Chaos*, 4, 4, 979–998, 1994.
14. J. F. Heagy, T. L. Carroll and L. M. Pecora. Desynchronization by periodic orbits. *Physical Review E*, 52, 2, R1253–R1256, 1995.
15. N. F. Rulkov. Images of synchronized chaos: Experiments with circuits. *Chaos: An Interdisciplinary Journal of Nonlinear Science*, 6, 3, 262–279, 1996.
16. L. M. Pecora, T. L. Carroll, G. A. Johnson, D. J. Mar and J. F. Heagy. Fundamentals of synchronization in chaotic systems, concepts, and applications. *Chaos: An Interdisciplinary Journal of Nonlinear Science*, 7, 4, 520–543, 1997.
17. G. Kolumbán, M. P. Kennedy and L. O. Chua. The role of synchronization in digital communication using chaos. I. Fundamentals of digital communications. *IEEE Transactions on Circuits and Systems I: Fundamental Theory and Applications*, 44, 10, 927–935, 1997.

18. J. Guare. Six Degrees of Separation: A Play. *Vintage*, 1990.
19. D. J. Watts and S. H. Strogatz. Collective dynamics of small–world networks. *Nature*, 393, 6684, 440–442, 1998.
20. S. Milgram. The Small–World Problem. *Psychology today*, 2, 1, 60–67, 1967.
21. V. Latora and M. Marchiori. Economic small–world behavior in weighted networks. *The European Physical Journal B – Condensed Matter and Complex Systems*, 32, 2, 249–263, 2003.
22. A. G. Soriano–Sánchez, C. Posadas–Castillo, M. A. Platas–Garza and D. A. Diaz–Romero. Performance improvement of chaotic encryption via energy and frequency location criteria. *Mathematics and Computers in Simulation*, 112, 14–27, 2015.
23. A. G. Soriano-Sánchez, C. Posadas-Castillo and M. A. Platas-Garza, C. Cruz-Hernández and R. M. López-Gutiérrez. Coupling strength computation for chaotic synchronization of complex networks with multi-scroll attractors. *Applied Mathematics and Computation*, 275, 305–316, 2016.
24. A. G. Soriano-Sánchez, C. Posadas-Castillo and M. A. Platas-Garza. Synchronization of Generalized Chua's Chaotic Oscillators in Small-world Topology. *Journal of Engineering Science and Technology Review*, 8, 2, 185–191, 2015.
25. F. C. Santos, J. F. Rodrigues and J. M. Pacheco. Epidemic spreading and cooperation dynamics on homogeneous small–world networks. *Physical Review E*, 72, 5, 056128, 2005.
26. Z. Wang, H. Zhang, and Z. Wang. Multiple effects of self-protection on the spreading of epidemics. *Chaos, Solitons & Fractals*, 61, 1–7, 2014.
27. O. Sporns. The human connectome: a complex network. *Annals of the New York Academy of Sciences*, 1224, 1, 109–125, 2011.
28. D. H. Zanette. Dynamics of rumor propagation on small-world networks. *Physical review E*, 65, 4, 041908, 2002.
29. N, Davey, B. Christianson and R. Adam. High capacity associative memories and small world networks. *Proceedings 2004 IEEE International Joint Conference on Neural Networks*, 1, 2004.
30. L. Guzmán–Vargas and R. Hernández–Pérez. Small–world topology and memory effects on decision time in opinion dynamics. *Physica A*, 372, 326–332, 2006.
31. X. F. Wang. Complex Networks: Topology, Dynamics and Synchronization. *International Journal of Bifurcation and Chaos*, 12, 5, 885–916, 2002.
32. X. F. Wang and G. Chen. Synchronization in small–world dynamical networks. *International Journal of Bifurcation and Chaos*, 12, 1, 187–192, 2002.
33. A. Barrat and M. Weigt. On the properties of small–world network models. *The European Physical Journal B – Condensed Matter and Complex Systems*, 13, 3, 547–560, 2000.
34. M. E. J. Newman and D. J. Watts. Renormalization group analysis of the small–world network model. *Physics Letters A*, 263, 4, 341–346, 1999.
35. M. E. J. Newman and D. J. Watts. Scaling and percolation in the small–world network model. *Physical Review E*, 60, 6, 7332–7342, 1999.
36. M. E. Yalçin, J. A. K. Suykens and J. P. L. Vandewalle. Cellular Neural Networks, Multi-Scroll Chaos and Synchronization. *World Scientific Publishing Co. Pte. Ltd.*, 50, Serie A, 2005.